

# KINETICS STUDIES OF REMOVAL OF REACTIVE RED 120 TEXTILE DYE FROM AQUEOUS SOLUTIONS USING JATROPHA CURCAS SHELLS

C.R. Gally<sup>1</sup>; E.C. Lima<sup>1</sup>; G.S. Reis<sup>1</sup>; M.J. Puchana<sup>1</sup>; M.A. Adebayo<sup>1</sup>; L.D.T. Prola<sup>1</sup>; E. Acayanka<sup>2</sup>; S. Laminsi<sup>2</sup>, P. Djifon<sup>2</sup>

<sup>1</sup> Instituto de Química, Universidade Federal do Rio Grande do Sul, UFRGS  
Av. Bento Gonçalves 9500, 91501-970, Porto Alegre, RS, Brasil

Telephone: (51) 3308 6302 – Fax: (51) 3308-7304 – Email: calinegally@hotmail.com

<sup>2</sup> Inorganic Chemistry Department, University of Yaoundé I, P.O. Box 812, Yaoundé, Cameroon.

**ABSTRACT:** The use of native *Jatropha curcas* (JN) and *Jatropha curcas* treated by non-thermal plasma (JP) as biosorbents for the removal of Reactive Red 120 (RR-120) dye from aqueous solutions was proposed in this work. *Jatropha curcas* is an abundant residue in the biocombustible industry. These biosorbents were characterized by infrared spectroscopy (FTIR), scanning electron microscopy (SEM), and by nitrogen adsorption/desorption curves. The effects of pH, shaking time and temperature on adsorption capacity were studied. In the acidic pH region (pH 2.0), the adsorption of the dye was favorable on JN and JP biosorbents. The maximum sorption capacity for adsorption of the dye occurred at 323 K attaining values of 40.94 and 65.63 mg g<sup>-1</sup> for JN and JP, respectively. Simulated dyehouse effluents were used to check the applicability of the proposed biosorbents for effluent treatment (removed 68.2 and 94.6%, for JN and JP, respectively) in a medium with high salt concentration.

**KEYWORDS:** *Jatropha curcas*; Reactive Red 120; biosorbent; effluent.

## 1. INTRODUCTION

The process of adsorption transfers the dyes from the aqueous effluent to a solid phase, significantly decreasing bioavailability of the dye to living organisms (Wang and Li, 2013). The decontaminated effluent can then be released to the environment (Machado et al., 2011, 2012).

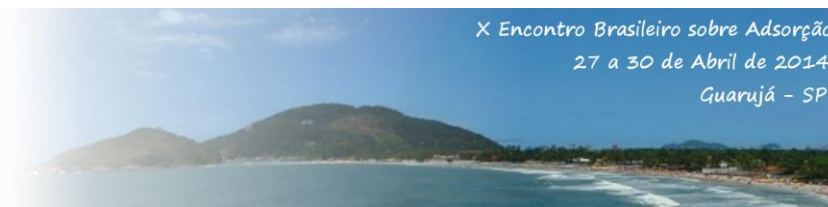
Activated carbon is one of the most employed adsorbents for dye removal from aqueous solution because of its excellent adsorption properties (Calvete et al., 2009, 2010; Cardoso et al., 2011c). However, the extensive use of activated carbon for dye removal from industrial effluents is expensive (Alencar et al., 2012a,b; Machado et al., 2012), due to its high initial and regeneration costs (Machado et al., 2011), thus limiting more extensive application in wastewater treatment. There is therefore a growing interest in finding alternative low cost adsorbents for removal of dyes from aqueous solution.

Although unmodified biosorbent could show good adsorption capacity, some chemical modifications on the biomass have been proposed recently to improve the maximum sorption capacity of biosorbents.

In the work was used biomass material using Gliding arc plasma type. *Jatropha curcas* was used as biosorbent in native form (JN) and also chemically modified by non-thermal plasma (JP) to removal of Reactive Red 120 textile dye from aqueous effluents.

*Jatropha curcas* is a multipurpose plant with many attributes and considerable potential, functional groups that are considerably different to those of activated materials, which may lead to greater adsorption potential of activated samples (Sricharoenchaikul, 2007).

Gliding arc plasma is a technique that takes its advantage to the presence of auto-generated reactive species like HO• and NO• radicals. The gliding electric discharge is obtained by blowing



an electric arc burning between diverging electrodes by axial gas flow (Czernichowski et al., 1996).

The plasma device has been used for the abatement of gaseous or liquid chemical pollutants (Burlica et al., 2004; Brisset et al., 2008; Laminsi et al., 2012). When humid air is selected as the ambient gas for discharges at atmospheric pressure, the resulting plasma was highly efficient for oxidizing because the resulting non-thermal plasma formed involves HO• as a result of electron (or/and photon) impact dissociation of water molecules present in the ambient gas at the liquid surface (Hnatiuc, 2002). In the present study, the use of non-thermal plasma for chemical modification of biosorbent is proposed.

## 2. MATERIAL AND METHODS

### 2.1 Solutions and reagents

Deionized water was used throughout the experiments for solution preparations. The Reactive Red 120 dye (RR-120) (C.I. 25810; C<sub>44</sub>H<sub>24</sub>Cl<sub>2</sub>N<sub>14</sub>O<sub>20</sub>S<sub>6</sub>Na<sub>6</sub>, 1469.98 g mol<sup>-1</sup>), was obtained from Sigma (Switzerland), as a commercially available textile dye, with 70% dye content, and it was used without further purification. RR-120 has six sulphonate groups. These groups have negative charges even in highly acidic solutions due to their pK<sub>a</sub> values being lower than zero (Roberts and Caserio, 1977). The stock solution of 5.00 g L<sup>-1</sup> was prepared by dissolving dye in distilled water to the concentration. The working solutions were obtained by diluting the dye stock solution to the required concentrations. The pH was adjusted using 0.10 mol L<sup>-1</sup> sodium hydroxide and/or 0.10 mol L<sup>-1</sup> hydrochloric acid solutions. The pH of the solutions was measured using a Schott Lab 850 set pH meter.

### 2.2 Biosorbent preparation and characterization

The *J. curcas* shell (JN) utilized in this work was provided by SADA Bioenergy and Agriculture Company Ltd., a unit of Jaíba, MG, Brazil. The Brazilian production of *J. curcas* is about 400,000 ton/year (50,000 ha with productivity of 8 ton/ha) (Gusmão, 2010).

About 32% of *J. curcas* correspond to the shell (128,000 ton/year of JN) (Gusmão, 2010). JN

was washed with tap water to remove dust, and then with deionized water. It was then dried at 70°C in an air-supplied oven for 8 h (Cardoso et al., 2011a,b). After this procedure, the JN was ground in a disk-mill and subsequently sieved. *J. curcas* of ≤ 106 µm diameter was used. This *J. curcas* shell seed was assigned as JN.

In order to increase the amount of RR-120 dye adsorbed by the JN biosorbent, the biomaterial was treated according to the procedure: a 50.0 g of JN was suspended in a 500.0 mL deionized water that was disposed normally to the axis of the water cooled glass reactor at a distance of about 50 mm from the electrodes tips. The solution was magnetically stirred and exposed to the plasma for 30 min. The gliding arc plasma forms when a suitable potential difference (10 kV; 160 mA) is applied between two (or more) diverging conductors.

The arc forms at the narrowest electrode gap by applying a suitable alternate or continuous potential difference between the conductors. The electrodes are laid out symmetrically around a gaseous jet (gas flow rate: 800 L h<sup>-1</sup>). The arc is pushed by the gas flow along the knife shaped electrodes to their tips: thus its length increases and its temperature decreases until it is short-circuited by a new arc and bursts in a quenched cold plasma cloud. The arc is thermal plasma, which favours the formation of active species and free radicals, which confer on plasma its particular chemical properties.

The plume of quenched plasma licks a target and its species react at the target-plasma interface. For this work, a half-open plasma reactor of the first generation reactor was used. After the discharge was switched off, the exposed mixture was centrifuged at 3600 rpm for 10 min, and the resulting biomass (JP) was washed several times with deionized water and dried at 70°C in the oven until constant weight. Afterwards, JP was kept in glass bottle for further use.

The particle sizes of the biosorbents were determined by sieve analysis. The JN and JP biosorbents were characterized using vibrational spectroscopy in the infrared region with Fourier Transform (FTIR) using a Spectrometer Shimadzu model IR Prestige 21 (Japan). The JN and JP samples and KBr were previously dried at 120°C for 8 h, and then they were stored in capped flasks and kept in a desiccator before the analysis. The spectra were obtained with a resolution of 4 cm<sup>-1</sup>

using 100 cumulative scans (Cardoso et al., 2011a,b).

The surface analyses and porosity were carried out with a volumetric adsorption analyzer, Nova 1000 (Quantachrome Instruments, USA), at 77 K (the boiling point of nitrogen). The samples were pre-treated at 473 K for 24 h under a nitrogen atmosphere in order to eliminate the moisture adsorbed on the surface of the solid sample. The samples were then submitted to conditions of 298 K in a vacuum, reaching the residual pressure of  $10^{-4}$  Pa. For area and pore calculations, the multi-point BET (Brunauer, Emmett and Teller) (Jacques et al., 2007a) and BJH (Barret, Joyner and Halenda) (Vaggetti et al., 2003) methods were used. The biosorbent samples were also analyzed with scanning electron microscopy (SEM; Jeol microscope, model JSM 6060) using an acceleration voltage of 10 kV and magnification ranging from  $200\times$  to  $5000\times$  (Jacques et al., 2007b).

The point of zero charge (pHpzc) of the biosorbent was determined by adding a 20.00 mL of  $0.050 \text{ mol L}^{-1}$  NaCl with a previously adjusted initial pH (the initial pH ( $\text{pH}_i$ ) values of the solutions were adjusted from 2.0 to 10.0 by adding  $0.10 \text{ mol L}^{-1}$  of HCl and NaOH) to several 50.0 mL cylindrical high-density polystyrene flasks containing 50.0 mg of the biosorbent, which were immediately securely capped.

The suspensions were shaken in an acclimatized shaker at 298 K and allowed to equilibrate for 48 h. The suspensions were then centrifuged at 10,000 rpm for 10 min to separate the biosorbent from the aqueous solution. The  $\text{pH}_i$  of the solutions were accurately measured using the solutions that had no contact with the solid biosorbent and the final pH ( $\text{pH}_f$ ) values of the supernatant after contact with the solid were recorded. The value of pHpzc is the point where the curve of  $\Delta\text{pH}$  ( $\text{pH}_f - \text{pH}_i$ ) versus  $\text{pH}_i$  crosses a line equal to zero (Calvete et al., 2009).

### 2.3. Batch biosorption studies

The batch biosorption studies for evaluation of the ability of JN and JP biosorbents to remove RR-120 dye from aqueous solutions were carried out in triplicate, using the batch contact biosorption method.

For these experiments, a 50.0 mg of biosorbent were placed in 50 mL cylindrical polypropylene flasks containing 20.0 mL of dye

solution ( $40\text{--}100.0 \text{ mg L}^{-1}$ ), which were agitated for an appropriate time (0.0833–24.00 h) using an acclimatized shaker at 298 K. pH of solution varied from 2.0 to 10.0. Subsequently, in order to separate the biosorbent from the aqueous solutions, the flasks were centrifuged at 10,000 rpm for 5 min using a Unicen M Herolab centrifuge (Stuttgart, Germany), and aliquots of the supernatant were properly diluted with an aqueous solution fixed at pH 2.0.

The final concentrations of the dyes remaining in the solution were quantified using a visible spectrophotometer (T90+ UV-VIS spectrophotometer; PG Instruments, London, England) fitted with quartz optical cells. Absorbance measurements were made at 534 nm, the maximum wavelength of RR-120 dye. The amount of dye taken up and the percentage of the dye removed by the biosorbents were calculated by using Equations (1) and (2), respectively:

$$q_e = \frac{(C_o - C_f)}{X} \quad (1)$$

$$\% \text{ Removal} = \frac{(C_o - C_f)}{C_o} \cdot 100 \quad (2)$$

In which  $q$  is the amount of dye adsorbed by the biosorbent ( $\text{mg g}^{-1}$ ),  $C_o$  is the initial dye concentration placed in contact with the biosorbent ( $\text{mg L}^{-1}$ ),  $C_f$  is the dye concentration ( $\text{mg L}^{-1}$ ) after the batch biosorption procedure,  $m$  is the mass of biosorbent (g) and  $V$  is the volume of dye solution (L).

The experiments of desorption were carried out according to the procedure: a  $50.0 \text{ mg L}^{-1}$  of RR-120 dye was shaken with 50.0 mg of JN and JP adsorbents for 1 h, then the loaded biosorbent was filtered using  $0.2 \mu\text{m}$  cellulose acetate and firstly washed with water to remove non-adsorbed dyes. Then, the dye adsorbed on the adsorbent was agitated with a 20.0 mL of: NaCl aqueous solutions ( $0.05\text{--}0.5 \text{ mol L}^{-1}$ ); acetone (10–50%) + water (90–50%), and acetone (10–50%) + 0.05 M NaCl (90–50%) for 15–60 min. The desorbed dyes were separated and estimated as described above.

### 2.4. Quality assurance and statistical evaluation of the kinetic and isotherm parameters



Blank tests were run in parallel and were corrected when necessary. All dye solutions were stored in glass bottles, which were cleaned by soaking in 1.4 mol L<sup>-1</sup> HNO<sub>3</sub> for 24 h (Barbosa et al., 1999), rinsing five times with deionized water, drying and storing them in a flow-hood. For analytical calibration, standard solutions with concentrations ranging from 5.00 to 100.0 mg L<sup>-1</sup> of the dyes were used, in parallel with a blank solution of water adjusted to pH 2.0.

The linear analytical calibration of the curve was furnished by the UVWin software of the T90+ PG Instruments spectrophotometer. The detection limit of the method, obtained with a signal/noise ratio of 3 (Lima et al., 1998b), was 0.19 mg L<sup>-1</sup> of RR-120. All the analytical measurements were performed in triplicate, and the precision of the standards was better than 3% (n = 3). In order to verify the accuracy of the RR-120 dye sample solutions during spectrophotometric measurements standards containing dyes at 40.0 mg L<sup>-1</sup> were employed as a quality control after every five determinations (Lima et al., 1998a).

The kinetic models were fitted by employing a nonlinear method, with successive interactions calculated by the Levenberg–Marquardt method; interactions were also calculated using the Simplex method, based on the nonlinear fitting facilities of the software Microcal Origin 9.0. In addition, the models were evaluated by a determination coefficient (R<sup>2</sup>), an adjusted determination coefficient (R<sup>2</sup><sub>adj</sub>), as well as by an error function (F<sub>error</sub>) (Calvete et al., 2010; Cardoso et al., 2012), which measured the differences in the amount of dye taken up by the biosorbent as predicted by the models and the actual q measured experimentally. R<sup>2</sup>, R<sup>2</sup><sub>adj</sub> and F<sub>error</sub> are given below, in Equations (3), (4) and (5), respectively:

$$R^2 = \left( \frac{\sum_i^n (q_{i,exp} - \bar{q}_{i,exp})^2 - \sum_i^n (q_{i,exp} - q_{i,model})^2}{\sum_i^n (q_{i,exp} - \bar{q}_{i,exp})^2} \right) \quad (03)$$

$$R_{adj}^2 = 1 - (1 - R^2) \cdot \left( \frac{n-1}{n-p} \right) \quad (04)$$

$$F_{error(\%)} = 100 \times \sqrt{\left( \frac{1}{n-p} \right) \cdot \sum_i^n \left( \frac{q_{i,exp} - q_{i,model}}{q_{i,exp}} \right)^2} \quad (05)$$

q<sub>i,model</sub> is each value of q predicted by the fitted model, q<sub>i,exp</sub> is each value of q measured

experimentally, q<sub>exp</sub> is the average of q experimentally measured, n is the number of experiments performed, and p is the number of parameters of the fitted model (Calvete et al., 2010).

## 2.5. Simulated dye-house effluent

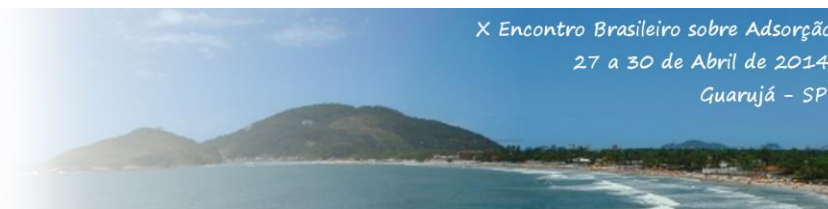
One synthetic dye-house effluent containing five representative reactive dyes usually used for colouring fibers and their corresponding auxiliary chemicals was prepared at pH 2.0, using a mixture of different dyes mostly used in the textile industry. According to the practical information obtained from a dye-house, typically 10–60% (Hessel et al., 2007) of reactive dyes and 100% of the dye bath auxiliaries remain in the spent dye bath, and its composition undergoes a 5–30-fold dilution during the subsequent washing and rinsing stages (Alencar et al., 2012b; Calvete et al., 2009). The concentrations of the dyes and auxiliary chemicals selected to imitate an exhausted dye bath are: Reactive Red 120 (λ<sub>max</sub> 534 nm) - 20.00 mg L<sup>-1</sup>; Cibacron Brilliant Yellow 3G-P (λ<sub>max</sub> 402 nm) - 5.00 mg L<sup>-1</sup>; Reactive Orange 16 (λ<sub>max</sub> 493 nm) - 5.00 mg L<sup>-1</sup>; Procion Blue MX-R (λ<sub>max</sub> 594 nm) 5.00 mg L<sup>-1</sup>; Reactive Black 5 (λ<sub>max</sub> 598 nm) - 5.00 mg L<sup>-1</sup>; Na<sub>2</sub>SO<sub>4</sub> - 80.0 mg L<sup>-1</sup>; NaCl - 80.0 mg L<sup>-1</sup>; Na<sub>2</sub>CO<sub>3</sub> - 50.0 mg L<sup>-1</sup>; CH<sub>3</sub>COONa - 50.0 mg L<sup>-1</sup>; CH<sub>3</sub>COOH - 600.0 mg L<sup>-1</sup> and pH 2.0. (Alencar et al., 2012b; Machado et al., 2011, 2012; Calvete et al., 2009; Cardoso et al., 2011c, 2012).

## 3. RESULTS AND DISCUSSION

### 3.1. Characterization of biosorbents

FTIR technique was used to examine the surface groups of JN and JP biosorbents and to identify the groups responsible for biosorption of the dye. Infrared spectra of the biosorbents were recorded in the range 4000–400 cm<sup>-1</sup>.

The JN and JP present the following FTIR bands: the broad band at 3366 and 3245 cm<sup>-1</sup> were assigned to O-H bond stretching for JN and JP, respectively (da Silva et al., 2011; Smith, 1999); the CH<sub>2</sub> stretching band observed at 2888 and 2900 cm<sup>-1</sup>, for JN and JP biosorbents, respectively (Smith, 1999; da Silva et al., 2011); a shoulder at 1725 cm<sup>-1</sup> (JN) and a sharp band at 1732 (JP) were assigned to carbonyl groups of carboxylic acid (Smith, 1999; da Silva et al., 2011); FTIR



vibrational bands at 1600 and 1613  $\text{cm}^{-1}$  were assigned to asymmetric stretching of carboxylate groups present in the lignocellulosic materials for JN and JP biosorbents, respectively (Jacques et al., 2007b; Smith, 1999); a band at 1404 for JN and a small band at 1431  $\text{cm}^{-1}$  are assigned to ring modes of aromatic ring (Cardoso et al., 2011a,b; Smith, 1999); the bands at 1317  $\text{cm}^{-1}$  (JN) and 1369 and 1320  $\text{cm}^{-1}$  (JP) are assigned to bending of CH groups of cellulose, hemicellulose and lignin (Smith, 1999); the bands at 1108 (JN) and 1156  $\text{cm}^{-1}$  (JP), were assigned to a C-O-C asymmetric stretch of ether groups of lignin (Alencar et al., 2012a; Smith, 1999). The intense FTIR band at 1023 (JN) and 1071 and 1013  $\text{cm}^{-1}$  (JP) are assigned to a C O stretch of primary alcohol of lignin (Alencar et al., 2012a; Smith, 1999).

It is noteworthy that in the region of 1460–1260  $\text{cm}^{-1}$  the FTIR bands of JP biosorbent are so small compared with the bands of JN. This feature may be related either to the radical addition or oxidation of the biomass surface:

In the first case, the plasma medium by the presence of free radicals (Moussa et al., 2005; Benstaali et al., 2002) should participate in electrophilic addition to organic  $\pi$  systems, as in photochemical reactions by addition of OH and/or NO<sub>x</sub> groups at double bonds and could justify the observe decrease of band at 1430  $\text{cm}^{-1}$ .

In the second case, since the plasma treatment induces the formation of long life oxidative species ( $E_0$  ( $\text{H}_2\text{O}_2/\text{H}_2\text{O}$ ) = 1.68 V/NHE; Doubla et al., 2007; Kamgang-Youbi et al., 2007), the surface functionalization should take place with oxidation of alkane group in carboxylic acid as shows by the remarkable increase of intensity of the JP band at 1732  $\text{cm}^{-1}$  (carboxylic group), indicating that the plasma source induced the formation of acidic groups on the lignocelluloses material.

The textural properties of JN and JP obtained by nitrogen adsorption/desorption curves were: superficial area ( $S_{\text{BET}}$ ), 6 and 15  $\text{m}^2 \text{g}^{-1}$ ; average pore diameter (BJH), 9 and 14 nm; and total pore volume, 0.16 and 0.28  $\text{cm}^3 \text{g}^{-1}$ , for JN and JP, respectively. These textural properties obtained for JP and JN are consistent with values of lignin–cellulosic materials (Alencar et al., 2012a,b; Ay et al., 2012; Subbaiah et al., 2011). The maximum diagonal length of RR-120 is 2.59

nm, the dimensions of the chemical molecule were calculated using ChemBio 3D Ultra version 11.0.).

The ratios of average pore diameter of the biosorbents to the maximum diagonal length of dye were 3.6 ( $\emptyset\text{JN}/\emptyset\text{RR-120}$ ) and 5.5 ( $\emptyset\text{JP}/\emptyset\text{RR-120}$ ). Therefore, the mesopores of JN could accommodate up to three molecules of RR-120 dye, and the mesopores of JP could accommodate up to five molecules of RR-120 dye.

The number of molecules that could be accommodated in each pore of the biosorbent, is considered large when compared with other adsorbents (de Menezes et al., 2012; Machado et al., 2011; Royer et al., 2010). The textural appearance of JN is quite different from JP biomaterial, which could be visualized by SEM images of these biosorbents.

The JN biosorbent is a fibrous material with some macropores (pore with  $\emptyset > 50$  nm). In addition, the JN fibrous material is apparently rougher than JP biosorbent. The treatment of fibrous JN material with plasma changed the textural appearance of the yielding material, obtaining a biomaterial in form of thin lignocellulose sheets.

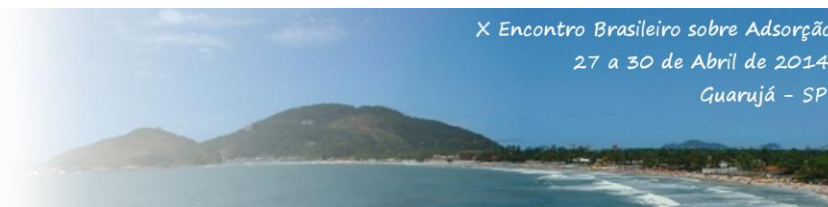
From analysis of the textural properties of JN and JP biosorbents, it could be inferred that these biosorbent materials predominantly contain a mixture of mesopores (pores with diameter ranging from 2 to 50 nm).

### 3.2. Effects of the particle size and pH of dye solution on biosorption

The effect of particle size of JN and JP biosorbents on the adsorption of 50.00  $\text{mg L}^{-1}$  of RR-120 dye was performed. It is expected that lower particle size would yield higher surface area and as a consequence (Wang and Li, 2007), it could give higher capacity of adsorption ( $q$ ).

For particles sizes lower than 106  $\mu\text{m}$  (106–90, 90–75, 75–63, and 63–53 $\mu\text{m}$ ), the values of the amount adsorbed of the dye per gram of both biosorbents was higher when compared with larger particles sizes (>300, 300–250, 250–180, 150–125, and 125–106  $\mu\text{m}$ ).

The effects of initial pH on percentage of removal of RR-120 dye solution (40  $\text{mg L}^{-1}$ ) using JN and JP biosorbents were evaluated within a pH range between 2 and 10. For JN biosorbent, the percentage of dye removed decreased markedly from 64.1% of dye removed at pH 2.0 to 9.1% removed at pH 7.0. For JP biosorbent, the



percentage of dye removed also decreased from 64.7% at pH 2.0 to less than 0.65% at pH 7.0. The pHPZC for both biosorbents confirm the ranges of optimal pH values for RR-120 removal from aqueous solutions.

The dissolved RR-120 dye is negatively charged in water solutions. The adsorption of the RR-120 dye takes place when the biosorbent present a positive surface charge. For JN, the electrostatic interaction occurs for  $\text{pH} < 5.85$ , and for JP this inter-action occurs for  $\text{pH} < 5.45$ . However, the lower the pH value from the  $\text{pH}_{\text{PZC}}$ , the more positive the surface of the biosorbent (Calvete et al., 2009). This behavior explains the high sorption capacity of JN and JP for both RR-120 dye at pH 2. The initial pH was fixed at 2.0.

### 3.3. Kinetic studies

Nonlinear pseudo-first order, pseudo-second order and general order kinetic biosorption models were used to evaluate the kinetics of biosorption of RR-120 dye using the JN and JP biosorbents. The kinetic parameters for the three kinetic models are listed in Table 2 (Conditions: temperature of 298 K; pH 2.0; mass of biosorbent 50.0 mg).

The  $q_e$  is the amount of adsorbate adsorbed by adsorbent at equilibrium in  $\text{mg g}^{-1}$ ;  $k_N$  represents the rate constant,  $k_1$  and  $k_2$  are the pseudo-first order and pseudo-second order rate constants, respectively;  $n$  is the order of adsorption in relation to the effective concentration of the adsorption active sites at the surface of adsorbent;  $k_{id}$  is intraparticle diffusion rate constant ( $\text{mg g}^{-1} \text{h}^{-0.5}$ ).

Taking into account that the experimental data were fitted using nonlinear kinetic models, an error function ( $F_{\text{error}}$ ) was used to evaluate the fit of the experimental data. The lower the  $F_{\text{error}}$ , the lower the difference in the calculated  $q$  and the experimental  $q$  (Calvete et al., 2009, 2010; Cardoso et al., 2011a,b, 2012; da Silva et al., 2011; de Menezes et al., 2012) (see Equation (5)). It should be pointed out that the  $F_{\text{error}}$  utilized in this work takes into account the number of fitted parameters ( $p$  term of Equation (5)), since it is reported (El-Khaiary et al., 2010; El-Khaiary and Malash, 2011) that the best fit of the results depends on the number of parameters a nonlinear equation presents. For this reason, the number of fitted parameters should be considered in the calculation of  $F_{\text{error}}$ .

In order to compare the different kinetic models, the  $F_{\text{error}}$  of individual model was divided

by the  $F_{\text{error}}$  of the minimum value ( $F_{\text{error}}$  ratio). It was found that the minimum  $F_{\text{error}}$  values were obtained with the general order kinetic model.

**Table 1.** Kinetic parameters for RR-120 removal using JN and JP biosorbent.

	JN		JP	
	50 $\text{mg L}^{-1}$	100 $\text{mg L}^{-1}$	50 $\text{mg L}^{-1}$	100 $\text{mg L}^{-1}$
<b>Pseudo-first order</b>				
$k_1$ ( $\text{h}^{-1}$ )	1.47	1.48	1.17	1.17
$q_e$ ( $\text{mg g}^{-1}$ )	10.03	12.33	12.26	20.98
$h_0$ ( $\text{mg g}^{-1} \text{h}^{-1}$ )	14.78	18.25	14.34	24.56
$R^2_{\text{adj}}$	0.975	0.975	0.968	0.968
Ferror (%)	10.64	10.19	12.71	12.65
<b>Pseudo-second order</b>				
$k_2$ ( $\text{g mg}^{-1} \text{h}^{-1}$ )	0.180	0.146	0.112	0.066
$q_e$ ( $\text{mg g}^{-1}$ )	10.75	13.22	13.30	22.77
$h_0$ ( $\text{mg g}^{-1} \text{h}^{-1}$ )	20.77	25.60	19.86	33.99
$R^2_{\text{adj}}$	0.999	0.999	0.997	0.997
Ferror (%)	2.53	2.01	4.02	3.97
<b>General order</b>				
$kN[\text{h}^{-1}(\text{g mg}^{-1})^n]$	0.0785	0.0640	0.0153	0.0063
$q_e$ ( $\text{mg g}^{-1}$ )	11.16	13.68	14.54	24.84
$N$	2.353	2.325	2.742	2.726
$h_0$ ( $\text{mg g}^{-1} \text{h}^{-1}$ )	22.90	28.02	23.58	40.21
$R^2_{\text{adj}}$	0.999	0.999	0.999	0.999
Ferror (%)	0.648	0.423	0.618	0.506
<b>Intraparticle</b>				
$k_{id}$ ( $\text{mg g}^{-1} \text{h}^{-0.5}$ ) <sup>a</sup>	1.393	1.687	2.088	3.424
$R_2$	0.996	0.994	0.999	0.993

The pseudo-first order kinetic model presented  $F_{\text{error}}$  ratio values ranging from 16.4 to 44.1 (JN) and 20.6 to 25.0 (JP). Similarly, for the pseudo-second order model, the  $F_{\text{error}}$  ratio values ranged from 3.9 to 4.2 (JN) and 6.5 to 7.9 (JP). These results clearly indicate that the general order kinetic model better explains the adsorption process of RR-120 dye using the JN and JP adsorbents. Taking into account that the general order kinetic equation presents different orders ( $n$ ) when the concentration of the adsorbed at the equilibrium ( $\text{mg g}^{-1}$ ), and  $n$  is the order of the kinetic model. It should be stressed that when  $n = 2$ , this equation is the same initial sorption rate as first introduced by Ho and McKay (1988). It was observed that by increasing the initial dye concentration, the initial sorption rate was increased for all kinetic models, as expected,



indicating that there is coherence with the experimental data (Alencar et al., 2012a,b; Cardoso et al., 2012; Machado et al., 2012).

Taking into cognisance that the kinetic data were better fitted by the general order kinetic model, meaning that the order of a biosorption process should follow the same logic as a chemical reaction and where the order is experimentally measured (Alencar et al., 2012a,b; Cardoso et al., 2012; Machado et al., 2012), instead of being previously stipulated by a given model, the more confident initial sorption rates ( $h_0$ ) were obtained by the general order kinetic model. It was observed that the kinetics of biosorption of RR-120 dye on JP biosorbent were faster than those obtained using JN biosorbent.

Considering the initial sorption rate ( $h_0$ ) of RR-120 dye taken up by JN and JP biosorbents, as obtained by the general order kinetic model, it was observed that  $h_0$  of JP biosorbent was increased by 2.97–43.5% compared to  $h_0$  obtained for JN biosorbent. It can be concluded that the plasma treatment of *J. curcas* shell promoted an increase in the macropore structure due to acid cleaning (Alencar et al., 2012a,b; Cardoso et al., 2011a,b), contributing to a faster diffusion of the RR-120 dye through the pores of the biosorbent, and also allowing higher amounts of the RR-120 dye to be adsorbed by the JP biosorbent.

In fact, any target exposed to reactive species flux created by non-thermal plasma in humid air is subjected to a progressive acidification. This is the direct consequence of the presence of  $\text{NO}^\bullet$  radical, which is in presence of  $\text{H}_2\text{O}$ , responsible for the formation of nitrous and nitric acid via  $\text{NO}_2$  (Moussa et al., 2005). The difference in  $h_0$  values, which is related to differences in the textural properties of the biosorbents after plasma treatment, is also in agreement with the results discussed above in the characterization of the biosorbents. The increase in the macropore structure of JP biosorbent should facilitate the diffusion of RR-120 dye molecules through the macropores (Cardoso et al., 2011a). As the adsorbate diffuses through the pores of the biosorbent, the dye could be adsorbed at the internal sites of the JP biomaterial; therefore both a fast kinetics of biosorption and higher sorption capacity of JP biosorbent were expected compared to JN biosorbent.

On the other hand, for the JN biosorbent, with a lower number of macropores, the

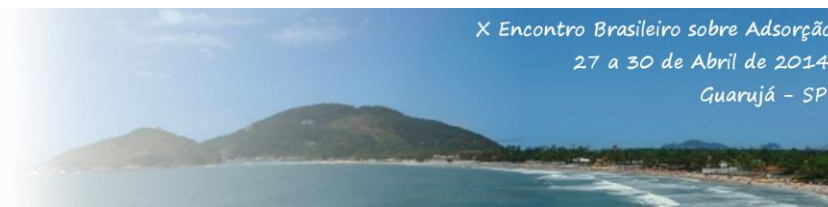
biosorption is limited to the external surface of the biosorbent, decreasing the total amount adsorbed (Alencar et al., 2012a,b; Cardoso et al., 2011a), and also leading to slower biosorption kinetics of RR-120 dye. The cavities generated in the JP biomaterial can be attributed to its treatment with plasma. The intra-particle diffusion model (Weber and Morris, 1963) was also used to verify the influence of mass transfer resistance on the binding of RR-120 dye to the biosorbents. The intra-particle diffusion constant,  $k_{id}$  ( $\text{mg g}^{-1} \text{h}^{-0.5}$ ), can be obtained from the slope of the plot of  $q_t$  ( $q_t$  is the amount of adsorbate adsorbed by adsorbent at a particular time,  $t$ , in  $\text{mg g}^{-1}$ ) versus the square root of the time. These results imply that the biosorption processes involved more than one sorption rate (Alencar et al., 2012a,b).

## 4. CONCLUSION

Native *J. curcas* shell (JN) and *J. curcas* shell treated with plasma (JP) are good alternative biosorbents for removal of the textile dye Reactive Red 120 (RR-120) from aqueous solutions. Four kinetic models were used to explain the biosorption, and the best fit was obtained with the general order kinetic model. However, the intra-particle diffusion model gave multiple linear regions, which suggested that biosorption may also be followed by multiple sorption rates. The minimum equilibration time of the dye was obtained after 8 h of contact between RR-120 dye and the JN and JP biosorbents. The maximum sorption capacity for adsorption of the dye occurred at 323 K attaining values of 40.94 and 65.63  $\text{mg g}^{-1}$  for JN and JP, respectively. For the treatment of simulated industrial textile effluents, the JN and JP biosorbents presented fair good performance, removing 68.2 and 94.6%, respectively, of a dye mixture in media containing high saline concentrations. The present study has showed that it is possible to significantly improve adsorbent properties of the biomass by exposure to non-thermal plasma.

## 5. REFERENCES

ALENCAR, W.S.; ACAYANKA, E.; LIMA, E.C.; ROYER, B.; DE SOUZA, F.E.; LAMEIRA, J.; ALVES, C.N. Application of *Mangifera indica* (mango) seeds as a biosorbent for removal of Victazol Orange 3R dye from aqueous solution and



- study of the biosorption mechanism. *Chem. Eng. J.* 209, 577–588, 2012a.
- ALENCAR, W.S., LIMA, E.C., ROYER, B., DOS SANTOS, B.D., CALVETE, T., DA SILVA, E.A., ALVES, C.N. Application of aqai stalks as biosorbents for the removal of the dye Procion Blue MX-R from aqueous solution. *Sep. Sci. Technol.* 47, 513–526, 2012b.
- BARBOSA JR., F., KRUG, F.J., LIMA, E.C. On-line coupling of electrochemical pre-concentration in tungsten coil electrothermal atomic absorption spectrometry for determination of lead in natural waters. *Spectrochim. Acta B* 54, 1155–1166, 1999.
- BRISSET, J.L., MOUSSA, D., DOUBLA, A., HNATIUC, E., HNATIUC, B., KAMGANG-YOUBI, G., HERRY, J.M., NAITALI, M., BELLON-FONTAINE, M.N. Chemical reactivity of dis-charges and temporal post-discharges in plasma treatment of aqueous media: examples of gliding arc discharge treated solutions. *Ind. Eng. Chem. Res.* 47, 5761–5781, 2008.
- CALVETE, T., LIMA, E.C., CARDOSO, N.F., DIAS, S.L.P., PAVAN, F.A. Application of carbon adsorbents prepared from the Brazilian-pine fruit shell for removal of Procion Red MX 3B from aqueous solution – kinetic, equilibrium, and thermo-dynamic studies. *Chem. Eng. J.* 155, 627–636, 2009.
- CALVETE, T., LIMA, E.C., CARDOSO, N.F., VAGHETTI, J.C.P., DIAS, S.L.P., PAVAN, F.A. Application of carbon adsorbents prepared from Brazilian-pine fruit shell for the removal of reactive orange 16 from aqueous solution: kinetic, equilibrium, and thermodynamic studies. *J. Environ. Manage.* 91, 1695–1706, 2011a.
- CARDOSO, N.F., LIMA, E.C., CALVETE, T., PINTO, I.S., AMAVISCA, C.V., FERNANDES, T.H.M., PINTO, R.B., ALENCAR, W.S. Application of aqai stalks as biosorbents for the removal of the dyes Reactive Black 5 and Reactive Orange 16 from aqueous solution. *J. Chem. Eng. Data* 56, 1857–1868, 2011a.
- CARDOSO, N.F., LIMA, E.C., PINTO, I.S., AMAVISCA, C.V., ROYER, B., PINTO, R.B., ALENCAR, W.S., PEREIRA, S.F.P. Application of cupuassu shell as biosorbent for the removal of textile dyes from aqueous solution. *J. Environ. Manage.* 92, 1237–1247, 2011b.
- CARDOSO, N.F., PINTO, R.B., LIMA, E.C., CALVETE, T., AMAVISCA, C.V., ROYER, B., CUNHA, M.L., FERNANDES, T.H.M., PINTO, I.S. Removal of remazol black B textile dye from aqueous solution by adsorption. *Desalination* 269, 92–103, 2011c.
- DA SILVA, L.G., RUGGIERO, R., GONTIJO, P.M., PINTO, R.B., ROYER, B., LIMA, E.C., FERNANDES, T.H.M., CALVETE, T. Adsorption of Brilliant Red 2BE dye from water solutions by a chemically modified sugarcane bagasse lignin. *Chem. Eng. J.* 168, 620–628, 2011.
- DE MENEZES, E.W., LIMA, E.C., ROYER, B., DE SOUZA, F.E., DOS SANTOS, B.D., GREGÓRIO, J.R., COSTA, T.M.H., GUSHIKEM, EL-KHAIARY, M.I., MALASH, G.F. Common data analysis errors in batch adsorption studies. *Hydrometallurgy* 105, 314–320, 2011.
- EL-KHAIARY, M.I., MALASH, G.F., HO, Y.S. On the use of linearized pseudo-second-order kinetic equations for modeling adsorption systems. *Desalination* 257, 93–101, 2010.
- MACHADO, F.M., BERGMANN, C.P., FERNANDES, T.H.M., LIMA, E.C., ROYER, B., CALVETE, T., FAGAN, S.B. Adsorption of Reactive Red M-2BE dye from water solutions by multi-walled carbon nanotubes and activated carbon. *J. Hazard. Mater.* 192, 1122–1131, 2011.
- MACHADO, F.M., BERGMANN, C.P., LIMA, E.C., ROYER, B., DE SOUZA, F.E., JAURIS, I.M., CALVETE, T., FAGAN, S.B. Adsorption of Reactive Blue 4 dye from water solutions by carbon nanotubes: experiment and theory. *Phys. Chem. Chem. Phys.* 14, 11139–11153, 2012.
- SMITH, B. *Infrared Spectral Interpretation. A Systematic Approach.* CRC Press, Boca Raton, 1999.
- SRICHAROENCHAikul, V; PECHYEN, C; AHT-ONG, D; ATONG, D. Preparation and Characterization of Activated Carbon from the Pyrolysis of Physic Nut (*Jatropha curcas* L.) Waste. *Energy & Fuels.* 22, 31–37, 2008.
- VAGHETTI, J.C.P., ZAT, M., BENTES, K.R.S., FERREIRA, L.S., BENVENUTTI, E.V., LIMA, E.C. 4-Phenylenediaminepropylsilica xerogel as a sorbent for copper determination in waters by slurry-sampling ETAAS. *J. Anal. At. Spectrom.* 18, 376–380, 2003.
- WANG, S., LI, H. Kinetic modelling and mechanism of dye adsorption on unburned carbon. *Dyes Pigments* 72, 308–314, 2007.
- WEBER JR., W.J., MORRIS, J.C. Kinetics of adsorption on carbon from solution. *J. Sanit. Eng. Div. Am. Soc. Civil Eng.* 89, 31–59, 1963.